



CrossMark
click for updates

Cite this: *RSC Adv.*, 2016, 6, 16239

Received 6th January 2016
Accepted 1st February 2016

DOI: 10.1039/c6ra00338a

www.rsc.org/advances

Application of group V polyoxometalate as an efficient base catalyst: a case study of decaniobate clusters†

Shun Hayashi,^a Seiji Yamazoe,^{ab} Kiichirou Koyasu^{ab} and Tatsuya Tsukuda^{*ab}

The base catalytic activity of the decaniobate cluster (TMA)₆[Nb₁₀O₂₈]·6H₂O (TMA⁺ = tetramethylammonium cation) was studied theoretically and experimentally. Density functional theory calculations showed that the oxygen atoms in the cluster are highly negatively charged and suggested the possibility that the cluster can act as a base catalyst. We demonstrated for the first time that [Nb₁₀O₂₈]⁶⁻ actually exhibits base catalytic activity for aldol-type condensation reactions including Knoevenagel and Claisen–Schmidt condensation reactions. The catalytic reactions proceeded under ambient conditions, suggesting that [Nb₁₀O₂₈]⁶⁻ holds promise as a practical strong base catalyst.

1. Introduction

A polyoxometalate (POM),¹ [M_xO_y]ⁿ⁻, is an anionic metal-oxide cluster that consists of a given number of [MO₆] octahedral units by sharing edges or corners. POMs have been widely used as catalysts, especially for acid-catalyzed, oxidation, and photocatalytic reactions.²⁻⁴ Recently, Mizuno and coworkers reported that [WO₄]²⁻ and [γ-HGeW₁₀O₃₆]⁷⁻ acted as base catalysts for CO₂ fixation⁵⁻⁷ and Knoevenagel condensation reaction,^{8,9} respectively. The base catalysis has been ascribed to the negativity of the oxygen atoms, mainly due to the high charge densities of the cluster.⁵ These studies have motivated us to develop stronger base catalysts based on POMs.

Our simple working hypothesis is that POM having more electronegative oxygen will exhibit stronger base catalysis. The $-n/y$ value of [M_xO_y]ⁿ⁻ represents a negative charge averaged over the oxygen atoms without assuming electronic charge transfer from metal to oxygen and thus provides a lower limit of the negativity of the oxygen atom. On the assumption that the $-n/y$ value gives a measure of the basicity of the POMs, group V POMs

(M = V, Nb, Ta) are more promising than group VI POM (M = Mo, W) for base catalysts. For example, polyoxoniobates (PONbs)^{10,11} such as hexaniobate ([Nb₆O₁₉]⁸⁻) and decaniobate ([Nb₁₀O₂₈]⁶⁻) cluster have more negative $-n/y$ values (−0.42 and −0.21, respectively) than polyoxotungstates (POWs) such as [HGeW₁₀O₃₆]⁷⁻ (−0.19), [W₁₀O₃₂]⁴⁻ (−0.13) and [W₆O₁₉]²⁻ (−0.11); although, [WO₄]²⁻ has a much more negative value of −0.50.

In order to test the hypothesis, we studied in this work homogeneous base catalysis of PONb. As an initial target, we focused on [Nb₁₀O₂₈]⁶⁻ rather than [Nb₆O₁₉]⁸⁻ although the latter has more negative $-n/y$ value. This is simply because the crystal structure of tetramethylammonium (TMA) salt, that can be dispersed in organic solvent, have been reported only for [Nb₁₀O₂₈]⁶⁻.¹² In this communication, we theoretically compared negative charges of oxygen atoms of [Nb₁₀O₂₈]⁶⁻ with those of POWs. Then, we applied (TMA)₆[Nb₁₀O₂₈]·6H₂O as homogeneous catalyst for aldol-type condensation reactions such as Knoevenagel and Claisen–Schmidt condensation reactions and revealed for the first time that it acted as a Brønsted base catalyst whose strength is comparable to superbases. This result will open up a new possibility of application of PONbs since their catalytic application has been limited to electrocatalysts¹³ and photocatalysts so far.¹⁴⁻¹⁷

2. Results and discussion

The structure of [Nb₁₀O₂₈]⁶⁻ was optimized by density functional theory (DFT) calculations. The structure obtained by optimization (Table S1†)¹⁸ reproduced that determined experimentally by single-crystal X-ray diffraction (XRD)¹² except that bond lengths were elongated by <3% relative to the experimental values. The localized charge of the oxygen atoms obtained by natural bond orbital (NBO) analysis is shown in Fig. 1; this gives a measure of the basicity of the individual oxygen atoms. The NBO charges of the oxygen atoms are much more negative than −0.21, which is the lower limit of the negativity without assuming electronic charge transfer between Nb and O. This result indicates electronic charge transfer from Nb to O

^aDepartment of Chemistry, School of Science, The University of Tokyo, 7-3-1 Hongo, Bunkyo-ku, Tokyo 113-0033, Japan. E-mail: tsukuda@chem.s.u-tokyo.ac.jp

^bElements Strategy Initiative for Catalysts and Batteries (ESICB), Kyoto University, Katsura, Kyoto 615-8520, Japan

† Electronic supplementary information (ESI) available. See DOI: 10.1039/c6ra00338a



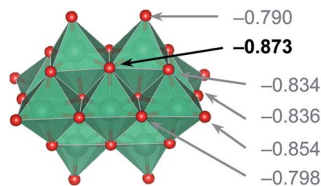


Fig. 1 Optimized structure and NBO charges of oxygen atoms in $[\text{Nb}_{10}\text{O}_{28}]^{6-}$ (D_{2h}).

atoms. Fig. 1 suggests that the four edge-sharing oxygen atoms of $[\text{Nb}_{10}\text{O}_{28}]^{6-}$ are the most active sites for base catalytic reaction.

The electronic charge of the most negative oxygen atom in $[\text{Nb}_{10}\text{O}_{28}]^{6-}$ (-0.873) was compared with those of other typical polyoxotungstates such as $[\text{W}_{10}\text{O}_{32}]^{4-}$, $[\text{W}_6\text{O}_{19}]^{2-}$, and $[\text{WO}_4]^{2-}$ (ref. 5) obtained from the same level of calculation (Fig. 2). The charge of the most negative oxygen atom in $[\text{Nb}_{10}\text{O}_{28}]^{6-}$ (-0.873) was much more negative than those of $[\text{W}_{10}\text{O}_{32}]^{4-}$ (-0.753) and $[\text{W}_6\text{O}_{19}]^{2-}$ (-0.721), but was slightly less negative than that of $[\text{WO}_4]^{2-}$ (-0.934). This comparison suggests that $[\text{Nb}_{10}\text{O}_{28}]^{6-}$ will show base catalysis as in the case of POWs reported so far.⁵⁻⁹

To test the base catalytic activity of $[\text{Nb}_{10}\text{O}_{28}]^{6-}$ cluster dispersed in organic solvent, we synthesized the TMA salt, $(\text{TMA})_6[\text{Nb}_{10}\text{O}_{28}] \cdot 6\text{H}_2\text{O}$, according to the reported method.¹² The synthesized product was characterized by powder XRD, negative-ion electrospray ionization mass spectrometry (ESI-MS), and elemental analysis. The powder XRD pattern of the product agreed well with that of $(\text{TMA})_6[\text{Nb}_{10}\text{O}_{28}] \cdot 6\text{H}_2\text{O}$ reported previously (Fig. 3).¹² The ESI-MS of the product in water-MeOH (1 : 1) exhibited a series of mass peaks assigned to $[\text{TMA}_x\text{H}_{(5-x)}\text{Nb}_{10}\text{O}_{28}]^-$ ($x = 2-5$) (Fig. 4). The elemental analysis of C, H, N, and Nb agreed with the calculated values for $[(\text{CH}_3)_4\text{N}]_6[\text{Nb}_{10}\text{O}_{28}] \cdot 6\text{H}_2\text{O}$ to an accuracy of $<0.5\%$ (calcd: C, 14.94; H, 4.36; N, 4.36; Nb, 48.2. Found: C, 14.75; H, 4.38; N, 4.27; Nb, 48.7). These results show that $(\text{TMA})_6[\text{Nb}_{10}\text{O}_{28}] \cdot 6\text{H}_2\text{O}$ was successfully synthesized.

We applied $(\text{TMA})_6[\text{Nb}_{10}\text{O}_{28}] \cdot 6\text{H}_2\text{O}$ as a homogeneous catalyst for the Knoevenagel condensation reaction. This is a fundamental coupling reaction to form carbon-carbon double bonds between active methylene compounds such as nitriles (donors) and carbonyl compounds (acceptors). The key step in

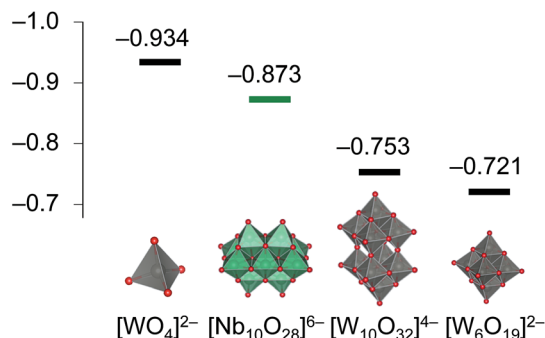


Fig. 2 NBO charges of the most negative oxygen atoms.

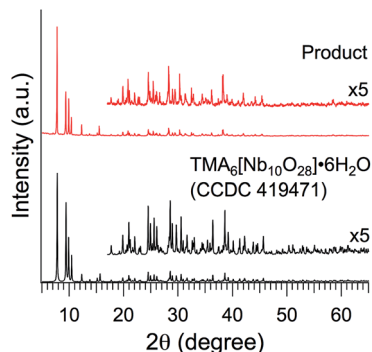


Fig. 3 Powder XRD pattern of the product and simulated pattern from reported crystal structure.¹²

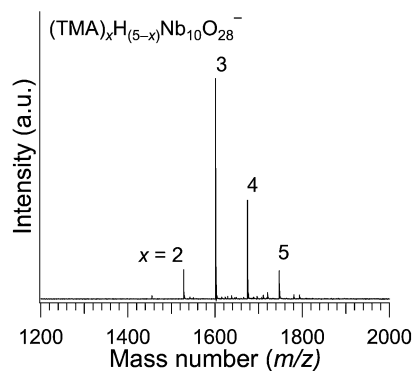


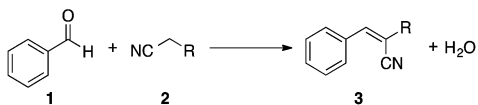
Fig. 4 Negative-ion ESI-MS of $(\text{TMA})_6[\text{Nb}_{10}\text{O}_{28}] \cdot 6\text{H}_2\text{O}$.

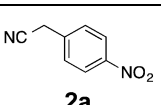
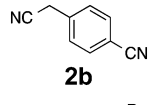
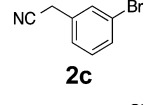
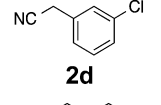
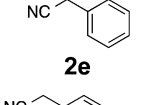
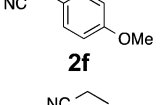
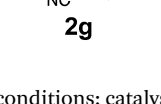
the reaction is proton abstraction from donors by base catalysts. We studied whether $(\text{TMA})_6[\text{Nb}_{10}\text{O}_{28}] \cdot 6\text{H}_2\text{O}$ catalyzed the coupling reaction between benzaldehyde (**1**) and various nitriles having different pK_a values. The results of the catalytic reactions are summarized in Table 1. $[\text{Nb}_{10}\text{O}_{28}]^{6-}$ cluster afforded in good yields coupling products with nitriles **2a** and **2b** (entries 1 and 2) whose pK_a values are 12.3 and 16.0 even at mild temperature $T = 313 \text{ K}$ (entries 1-1 and 2-1). Negative-ion ESI-MS of the catalyst after the reaction (entry 2-1) exhibited a series of mass peaks of $[\text{TMA}_x\text{H}_{(5-x)}\text{Nb}_{10}\text{O}_{28}]^-$ ($x = 1-3$) (Fig. S1†),¹⁸ suggesting that the catalysts did not decompose. Turnover frequencies for these reactions (entries 1-2 and 2-2) were calculated to be 66 and 28 h^{-1} at 343 K, respectively, from the kinetic data (Fig. S2†).¹⁸ $[\text{Nb}_{10}\text{O}_{28}]^{6-}$ cluster showed base catalytic activity for nitriles **2c** ($\text{pK}_a = 19.4$, entry 3), **2d** ($\text{pK}_a = 19.5$, entry 4), **2e** ($\text{pK}_a = 21.9$, entry 5) and **2f** ($\text{pK}_a = 23.8$, entry 6), although the yields gradually decreased with an increase in the pK_a values of the nitriles. However, $[\text{Nb}_{10}\text{O}_{28}]^{6-}$ cluster did not show any activity for the reaction of **2g** ($\text{pK}_a = 32.5$, entry 7).

Catalytic activity of $(\text{TMA})_6[\text{Nb}_{10}\text{O}_{28}] \cdot 6\text{H}_2\text{O}$ for Claisen-Schmidt condensation reaction between **1** and acetophenone (**2h**, $\text{pK}_a = 24.7$) was also studied. As shown in Scheme 1, $[\text{Nb}_{10}\text{O}_{28}]^{6-}$ also acted as a homogeneous base catalyst for Claisen-Schmidt condensation.

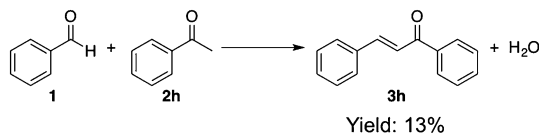
Although the yields of the reactions with **2f** ($\text{pK}_a = 23.8$) and **2h** ($\text{pK}_a = 24.7$) were low compared to typical base catalysts such



Table 1 Knoevenagel condensation catalyzed by $(\text{TMA})_6[\text{Nb}_{10}\text{O}_{28}] \cdot 6\text{H}_2\text{O}^a$


Entry	Donor	pK_a	Temp. (K)	Yield (%)
1-1		12.3	313	61
1-2			343	88
2-1		16.0	313	77
2-2			343	88
3		19.4	343	61
4		19.5	343	39
5		21.9	343	35
6		23.8	343	8
7		32.5	343	0

^a Reaction conditions: catalyst (1 mol% with respect to 1), 1 (1.0 mmol), 2 (1.0 mmol), MeOH 1 mL, 343 K, 24 h.

**Scheme 1** Claisen-Schmidt condensation catalyzed by $(\text{TMA})_6[\text{Nb}_{10}\text{O}_{28}] \cdot 6\text{H}_2\text{O}$. ^aReaction conditions: catalyst (1 mol% with respect to 1), 1 (1.0 mmol), 2 (1.0 mmol), MeOH 1 mL, 343 K, 24 h.

as hydroxide and alkoxide,^{19,20} the fact that $[\text{Nb}_{10}\text{O}_{28}]^{6-}$ cluster could activate less acidic nitriles indicated its strong basicity. To the best of our knowledge, $[\text{Nb}_{10}\text{O}_{28}]^{6-}$ cluster is the first example of a strong base catalyst that can activate **2f** and **2h** among various POMs. The base strength of $[\text{Nb}_{10}\text{O}_{28}]^{6-}$ is as high as 24.7 if we assume that the base strength of a catalyst is comparable to the pK_a values of methylene groups from which protons can be abstracted. This value is comparable to those of superbases, whose base strengths are defined to be larger than 26. However, those superbases are generally very sensitive to water and CO_2 and exhibit strong basicities only under rigorously controlled conditions.²¹ In contrast, $[\text{Nb}_{10}\text{O}_{28}]^{6-}$ cluster

showed base catalysis even when it was used in non-hydrated solvent under ambient conditions. This novel feature suggests that the PONbs hold promise as a practical strong base catalyst.

3. Conclusions

We have reported for the first time that decaniobate cluster $[\text{Nb}_{10}\text{O}_{28}]^{6-}$ acts as a strong and homogeneous base catalyst for Knoevenagel condensation reaction of benzaldehyde and *p*-methoxyphenylacetonitrile ($\text{pK}_a = 23.8$) and Claisen-Schmidt condensation reaction of benzaldehyde and acetophenone ($\text{pK}_a = 24.7$). This high catalytic activity is associated with the large negative charge on the oxygen sites (-0.79 to -0.87) originating mainly from the large total negative charge on the cluster.

4. Experiment and theory

4.1. Density functional theory calculations

DFT calculations were conducted using the Gaussian 09 program.²² The structure of $[\text{Nb}_{10}\text{O}_{28}]^{6-}$ was optimized at the level of B3LYP/6-31G++(d). The absence of imaginary frequencies was confirmed from vibrational analysis. Natural bond orbital (NBO) analysis was conducted to obtain localized charge on the oxygen atoms.

4.2. Chemicals

Niobic acid was supplied from CBMM ($\text{Nb}_2\text{O}_5 \cdot n\text{H}_2\text{O}$, water 20% w/w). Tetramethylammonium hydroxide pentahydrate (TCI, 97%), benzaldehyde (Wako, 98%), 4-nitrobenzyl cyanide (TCI, 98%), 4-cyanophenylacetonitrile (Aldrich, 97%), 3-bromobenzyl cyanide (TCI, 98%), *m*-chlorobenzyl cyanide (Wako, 98%), phenylacetonitrile (Wako, 98%), 4-methoxyphenylacetonitrile (Aldrich, 97%), propionitrile (Wako, 98%), and acetophenone (Wako, 98.5%) were used without further purification. Deionized water (Milli-Q, >18 MΩ cm) was used in all experiments.

4.3. Synthesis

$(\text{TMA})_6[\text{Nb}_{10}\text{O}_{28}] \cdot 6\text{H}_2\text{O}$ was synthesized according to the literature procedure.¹² In an autoclave, niobic acid ($\text{Nb}_2\text{O}_5 \cdot n\text{H}_2\text{O}$, water 20% w/w, 3.00 g, 9.02 mmol) was mixed with 30 mL of EtOH solution of tetramethylammonium hydroxide (3.60 g, 19.9 mmol). The autoclave was heated at 120 °C for 18 h. After the reaction, the orange solution was removed and a white precipitate was collected by centrifugation. The precipitate was washed with EtOH (150 mL) and acetone (150 mL) and dried well. The crude product was dissolved into 50 mL of MeOH and centrifuged to remove unreacted niobic acid. The solution was concentrated into 15 mL by evaporation and separated into three vials. Recrystallization was conducted by adding 20 mL of acetone slowly to each solution to form a second layer. Typical yield was 2.01 g (1.04 mmol, 58% based on Nb).

4.4. Characterization

The powder XRD pattern was collected with a Rigaku SmartLab 3 using nickel-filtered $\text{Cu-K}\alpha$ radiation. Negative-ion ESI-MS was measured with a JEOL JMS-T100LP AccuTOF LC-plus. $(\text{TMA})_6$



$[\text{Nb}_{10}\text{O}_{28}] \cdot 6\text{H}_2\text{O}$ was dissolved into water–MeOH (1 : 1, 1 mg mL^{-1}) and electrosprayed at a bias voltage of -2 kV. The mass spectrum was calibrated by using $\text{Cs}_n\text{I}_{(n+1)}^-$ clusters generated from CsI solution as a reference. Elemental analysis for C, H, and N was conducted with an Elementar vario MICRO cube. ICP-AES analysis for Nb was performed with a Thermo Scientific iCAP DUO-6300 at a wavelength of 309.4 nm. GC analysis was conducted with a Shimadzu GC-2014 with a Restek Rtx-1 (internal diameter = 0.53 mm, length = 30 m) capillary column, and GC-MS analysis was conducted with a Shimadzu GCMS-QP2010 Ultra with a Restek Rtx-1 (internal diameter = 0.32 mm, length = 30 m) capillary column at an ionization voltage of 70 eV.

4.5. Catalytic test

Benzaldehyde (1, 1.0 mmol), nitrile or acetophenone (2, 1.0 mmol), and biphenyl (internal standard, ca. 0.1 mmol) were dissolved into MeOH, and $(\text{TMA})_6[\text{Nb}_{10}\text{O}_{28}] \cdot 6\text{H}_2\text{O}$ (10 μmol , 1 mol%) was added to start the reaction. The reaction mixture was stirred for 24 h and then analysed by GC and GC-MS.

Acknowledgements

We thank Dr Naoko Nonose (National Institute of Advanced Industrial Science and Technology; AIST) for preliminary ICP analysis and Dr Noritaka Mizuno, Dr Kazuya Yamaguchi, and Dr Kosuke Suzuki (The University of Tokyo) for fruitful discussions. This research was financially supported by the Elements Strategy Initiative for Catalysis and Batteries (ESICB) and by a Grant-in-Aid for Scientific Research (No. 24750210) from the Ministry of Education, Culture, Sports, Science and Technology (MEXT) of Japan.

Notes and references

- 1 D. Long, R. Tsunashima and L. Cronin, *Angew. Chem., Int. Ed.*, 2010, **49**, 1736.
- 2 C. L. Hill and C. M. Prosser-McCartha, *Coord. Chem. Rev.*, 1995, **143**, 407.
- 3 I. V. Kozhevnikov, *Chem. Rev.*, 1998, **98**, 171.
- 4 N. Mizuno and M. Misono, *Chem. Rev.*, 1998, **98**, 199.
- 5 T. Kimura, K. Kamata and N. Mizuno, *Angew. Chem., Int. Ed.*, 2012, **51**, 6700.
- 6 T. Kimura, H. Sunaba, K. Kamata and N. Mizuno, *Inorg. Chem.*, 2012, **51**, 13001.
- 7 K. Kamata, T. Kimura, H. Sunaba and N. Mizuno, *Catal. Today*, 2014, **226**, 160.
- 8 K. Sugahara, T. Kimura, K. Kamata, K. Yamaguchi and N. Mizuno, *Chem. Commun.*, 2012, **48**, 8422.
- 9 K. Sugahara, N. Satake, K. Kamata, T. Nakajima and N. Mizuno, *Angew. Chem., Int. Ed.*, 2014, **53**, 13248.
- 10 M. Nyman, *Dalton Trans.*, 2011, **40**, 8049.
- 11 H. Wu, Z. Zhang, Y. Li, X. Wang and E. Wang, *CrystEngComm*, 2015, **17**, 6261.
- 12 C. A. Ohlin, E. M. Villa and W. H. Casey, *Inorg. Chim. Acta*, 2009, **362**, 1391.
- 13 Y. Ye, C. Chen, H. Feng, J. Zhou, J. Ma, J. Chen, J. Yuan, L. Kong and Z. Qian, *Open J. Inorg. Chem.*, 2013, **3**, 59.
- 14 L. Shen, Y. Xu, Y. Gao, F. Cui and C. Hu, *J. Mol. Struct.*, 2009, **934**, 37.
- 15 Z. Zhang, Q. Lin, D. Kurunthu, T. Wu, F. Zuo, S. Zheng, C. J. Bardeen, X. Bu and P. Feng, *J. Am. Chem. Soc.*, 2011, **133**, 6934.
- 16 Z. Wang, H. Tan, W. Chen, Y. Li and E. Wang, *Dalton Trans.*, 2012, **41**, 9882.
- 17 P. Huang, C. Qin, Z. Su, Y. Xing, X. Wang, K. Shao, Y. Lan and E. Wang, *J. Am. Chem. Soc.*, 2012, **134**, 14004.
- 18 See ESI†
- 19 B. A. Bhat, K. L. Dhar, S. C. Puri, A. K. Saxena, M. Shanmugavel and G. N. Qazi, *Bioorg. Med. Chem. Lett.*, 2005, **15**, 3177.
- 20 A. Ramirez-Rodríguez, J. M. Méndez, C. C. Jiménez, F. León and A. Vazquez, *Synthesis*, 2012, **44**, 3321.
- 21 L. Chen, J. Zhao, S. Yin and C. Au, *RSC Adv.*, 2013, **3**, 3799.
- 22 M. J. Frisch, G. W. Trucks, H. B. Schlegel, G. E. Scuseria, M. A. Robb, J. R. Cheeseman, G. Scalmani, V. Barone, B. Mennucci, G. A. Petersson, *et al.*, *Gaussian 09, Revision D.01*, Gaussian, Inc., Wallingford CT, 2013.

